JOURNAL OF OPTOELECTRONICS AND ADVANCED MATERIALS Vol. 8, No. 2, April 2006, p. 425 - 438

Invited Lecture

Materials and structures for semiconductor spintronics

V. G. KANTSER
International Laboratory of Superconductivity and Solid State Electronics of the Academy of Sciences of Moldova Rep Academiei str., 5, Chisinau, MD 2028, Moldova Rep.

The objective of this paper is to present a review of the recent results concerning the new concepts and achievements in the area of semiconductor spintronics, which has greatly emerged last years. Development of this field of semiconductor and magnetic physics is largely determined by the progress in synthesis of new materials and low dimensional structures, which are inherent to obtain functional spintronic devices. Some recent approaches for materials and structure development in the area of spin polarized carrier states and flow formation as well as spin injection is highlighted. In particular, the spintronics rout of II-VI, III-V and IV-VI ferromagnetic semiconductor compounds and structures is analyzed. Several methods and structures for spin manipulation and for testing spin parameters of carriers are presented underlying the role of spin-orbital interaction. The novel spintronics phenomenon - Spin Hall Effect (SHE) - is reviewed. New peculiarities of SHE, induced by interband interaction of heavy and light holes through optical like displacements, are studied in p-doped semiconductors.

(Received January 18, 2006; accepted March 23, 2006)

Keywords: Spintronics, Semiconductor heterostructures, Magnetic materials, Spin-orbit interaction, Spin hall effect

1. General considerations on spintronics

In order to perform different specific functionality such as signal detecting, processing, light emission etc. existing semiconductor electronic and photonic devices utilize the charge on carriers. Spintronics or spin-dependent electronics combines the intrinsic fundamental attributes of solid-state carriers – charge and spin [1]. From the classical point of view the spin is considered as an angular momentum, which by the rotating of charge induces a magnetic moment. However in contrast to a macroscopic angular momentum the spin is quantized and has two different (opposite) directions with the axis of quantization given by an external magnetic field. Therefore, whereas the carrier charge has a constant value and local changes of charge can only happen via a current , the spin of an electron can have two different values (spin-up and spin-down) and they can be ''flipped'' from one value to the other. This attribute provides the local creation of a spin population without a current (in comparison to a charge) but at the same time a spin population can vanish over time, while a charge population in the absence of a current cannot.

These specific peculiarities of the carrier spin in comparison with its charge have revealed a lot of fundamental problems:

1. What is an effective way to polarize a spin system?
2. How long is the system able to remember its spin orientation?
3. What are the mechanisms of the interaction between the particle spin and its solid- state environments?
4. How can spin be detected?

The basic concept of spintronics is the manipulation of carrier spin, in contrast to mainstream electronics in which the spin of the electron is ignored. Adding the spin degree of freedom provides new effects, new capabilities and new functionalities. Taking into account that the spin attribute is the basis of magnetism an indirect way of spin manipulation can be provided by magnetization. However there are two major obstacles. The first is related to the mechanism of magnetic properties modification, which until the mid-1980s was possible only via the magnetic field, using inductive pickup coils like in tape storage or computer disk applications. The second impediment is the equilibrium nature of magnetism in ferromagnets. The first obstacles have been overcome at the end of eighties, when the effect of giant magnetoresistance (GMR) was discovered in layered structures of ferromagnetic materials [2]. At present there are yet several devices working on the basis of the giant and recently tunneling (TMR) magnetoresistance principles. However, in metal-based devices high values for GMR and TMR can only be achieved when the thickness of the nonmagnetic material is only a few Angströms, a fact which limits the device resistance to fractions of an Ohm and is incompatible with existing CMOS technology. Furthermore, these small dimensions leave no tool for the manipulation of the spin. Therefore despite some practical achievements of metal magnetoelectronics the transition to semiconductor material basis was challenging. Indeed in 1990 a new concept for a semiconductor device for spin manipulation was published by Datta and Das [3], in which a spin-polarized current through a semiconductor can be modulated by an electrostatic gate via the spin-orbit coupling. This device is known as the Datta-transistor. The authors claimed that the spin-polarized current should be

obtained by using a GMR-like geometry with ferromagnetic metal contacts on a semiconductor mesa.

After Datta and Das seminal paper [3] experimental and theoretical efforts aiming at the implementation of the spin-dependent functions into the semiconductor (or hybrid metal-semiconductor) structures [4,5] have an exponential increase. However, despite strong influence of the achievements in semiconductor spintronics development the mail driven forces in its present emerging investigations are related to reaching the scale-down limit of the corresponding Moore's law of microelectronics in the near future. Fig. 1 illustrates the anticipated technology nodes for the semiconductor industry development following the Semiconductor Industry Association and International Technology Roadmap for Semiconductors [6]. The dashed wall in Fig. 1 is the boundary at which there are no known solutions for further development of semiconductor industry and therefore a cardinal research breakthrough is expected.

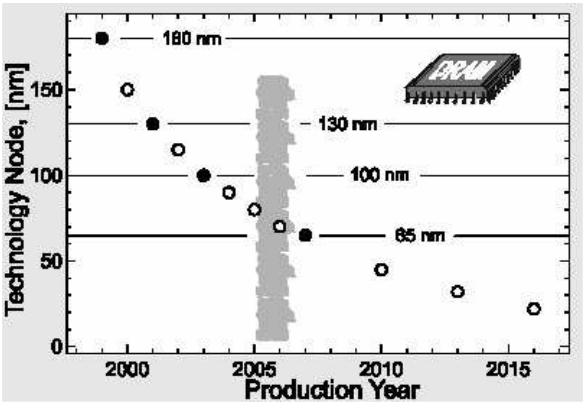

Fig. 1. Evolution of technology miniaturization for the traditional electronic devices [6].

In such circumstances the new concepts and principles in electronic device architectures are a major challenge of solid-state physics. Last years new approaches for future microelectronics have been suggested:

– Bottom-up approach to fabrication;

– Integration of function in devices;

– Change in characteristics of information carrier;

– Bioelectronics, polymer electronics, molecular electronics, spintronics.

One of such proposals in the underlined list is the spintronic one, which is considered among the more promising from the following reasons:

- higher level of device integration
- faster data manipulation
- lower power consumption
- current applications are based on the older concept of magnetoelectronics (tunnel, giant) magnetoresistance effects.

Development of this emerging field of semiconductor spin electronics (spintronics) is largely determined by the progress in synthesis of new materials and low dimensional structures, which are inherent to obtain functional spintronic devices. Current activities are devoted to obtain semiconductor ferromagnetic at room temperature, and to grow materials and structures with spin properties controlled and monitored by means of electrical, magnetical and optical methods [7-10]. In order to achieve a significant progress in semiconductor spin electronics it is necessary to put forward a complex approach, in which growth techniques of high quality materials are developed in parallel with experimental and theoretical analysis of spin-dependent material parameters, spin interactions and spin-dependent electronic structures of spintronic semiconductors. There are two main reasons for this:

1) Semiconductor-based spintronics could combine storage, detection, logic and communication capabilities on a single chip to produce a multifunctional device that could replace several components.

2) Semiconductors offer a greater wealth of possibilities to create and to manipulate the nonequilibrium spin by transport, optical, and resonance methods (as well as their combination).

There are four essential requirements for implementing a semiconductor spintronics principles in devices:

1. Efficient electrical injection of spin-polarised carriers into semiconductors.
2. Adequate spin diffusion lengths and lifetimes for transport in the device.
3. Effective control and manipulation of the spin system.
4. Efficient detection of the spin system determine the output.

The main goal of the spintronics is to create the flows of spins or spin polarised currents and to use them for signal processing, transmission, storage, detection etc. The most proposed until schemes and principles of semiconductor spintronics devices include as a component part the subsystem of formation of carrier assemble in spin-up or spin-down state and its transfer (injection) in the active zone of spin manipulation of the devices. The approaches developed and tested for such purposes in general can be divided into two main categories:

- *hybrid ferromagnetic/non-magnetic heterostructures*
- *all-semiconductor nonmagnetic heterostructures.*

In Section 2 of the paper we review some recent material and structure development in the area of spin polarized carrier state and flow formation as well as spin injection. Analyzing the non-magnetic approaches the spintronics properties of semiconductor structures with buried electrical polarization like GaN or strained structures will be considered. In particular, the tunnel characteristics of an symmetric barrier structure with incorporated electrical polarization will be shown to become to spin-dependent [11].

The ability to control and manipulate the electron spin requires efficient mechanisms of the spin splitting of the electronic states in the active spintronic structure part, of the spin dependent transport and optical characteristic modification in the controllable way under corresponding

external intervention. Many approaches have been proposed to achieve control of the electron spin degree of freedom using ferromagnetic materials, external electric and magnetic fields, optical excitation, etc. [7-10]. These external factors are channelled to act on the carrier spin through one of the following interactions:

- *Magnetic interaction*
- *Spin-orbit interaction (SOI)*
- *Exchange interaction*
- *Hyperfine interaction with nuclear spins.*

SOI is considered to be the main channel for spin manipulation due to:

- comparatively large magnitude;
- possibilities of using the electric fields, gates, optical phenomena and others for modification of spin states.

SOI arises as a result of the magnetic moment of the spin coupling to its orbital degree of freedom. When an electron is moving in a static electric field, in the rest frame of the electron the original static electric field transforms into a field that has also a magnetic field component

$$\vec{B}_{\text{eff}}(x) = \left(\vec{v}\times\vec{E}(x)\right)/c$$

$$H_{SO}(\vec{r}) = \frac{e\hbar}{4m_0c^2}\vec{\sigma}\left(\vec{E}(\vec{r})\times\vec{v}\right)$$

Zeeman like interaction of magnetic moment of the electron with this field leads to SOI. Thus SOI has a relativistic nature and is enough week for an electron in the vacuum [12]. At the same time from the quantum mechanical point of view SOI is generated by the interband coupling of electron like and positron like branches of the electron spectrum and its weakness is related to large Dirac gap $2m_0c^2$. In semiconductor materials and structures within the approximation of two-band model the equations are similar to a Dirac equation but with the forbidden gap E_g instead of the Dirac gap $2m_0c^2$ [2]. Therefore H_{SO} after the reduction to one band model becomes

$$H_{SO} = \frac{1}{2m_0}\left[\vec{p}\times\hbar\vec{\nabla}\left(\frac{V_{ext}}{2E_g}\right)\right]\vec{\sigma}$$

This simplest analysis suggests that the first way to have efficient spintronic materials is to build semiconductors with narrow gap. However depending on technological reasons and method of spin manipulation there is a compromise between the up and down limit of the gap value. In this situation other mechanisms of the SOI enhancement are necessary. Such possibility appears in semiconductor structures with buried confinement electrostatic potential due to various factors influencing the motion of the carriers. This leads to new terms in SOI such as Dresselhaus and Rashba ones, which are more frequently explored for different spintronics functional applications [1,12], because they can be tailored by structure engineering.

The above mentioned mechanisms of SOI stem from the electron orbital motion and are related to the 3D spatial angular momentum. At the same time there is angular momentum related to the generators of so-called Lorentz boosts [13]. Recently [14] it was shown that, to a charged system with nonzero space-time components of 4D angular momentum tensor (i.e. the generators of Lorentz boost) there may correspond an electric moment similar to a charged system with nonzero purely spatial components of 4D angular momentum tensor (i.e. the generators of 3D spatial rotation) there may correspond a magnetic moment. This new fundamental quantum attribute of the electron in vacuum [14] - *induced* electric moment must have a lot of richer manifestations in crystals, in particular in semiconductor materials and heterostructures.

In such a way due to this and taking into account the interband origin of the SOI in semiconductor materials and structures new terms of SOI can appear. For this it is important to design materials and structures with new types of interband coupling. One of such interband interactions appears through phonons. First type of SOI terms appears in the result of interband-deformation potential interactions through acoustic phonons and one of the variants has been considered recently [15] for p-doped semiconductors. It was shown that this SOI induces piezo-magneto-electric effects with new functionality for spintronics.

Another type of SOI terms appears in the result of interband-deformation potential interactions through optical phonons. One of the manifestations of this mechanism of SOI generation is related to electrical polarization appearing in spontaneous way due to the atomic displacements of two sublattices of semiconductor compound or due to piezoelectric effect induced by strain. In the context of interface electronic states in semiconductor heterostructures a variant of inteband interaction electrical polarization has been studied firstly in papers [16,17] in the frame of two band model of semiconductors with similar conduction and valence bands (like PbTe). In the context of the spintronics this interaction was shown to lead even in the simplest two-band to the appearance of new SOI terms [18]. Several aspects of methods to control carrier spin and to test spin parameters and dynamics are highlighted in Section 3.

Section 4 of the paper includes some results dealing with the new discovered spintronics phenomenon - spin Hall effect (SHE) [19,20]. The geometrical structure of the intrinsic SHE is such that for an electric field applied, for example, on the z direction, a y-polarized dissipationless spin current will flow in the x direction. The following macroscopic relation can summarize the electric field induced spin current $J_j^i = \sigma_s \varepsilon_{ijk} E_k$. The extrinsic SHE is related to skew-scattering mechanism [21] and is based on asymmetric scattering of spin-up and spin-down electrons from a random impurity potential that includes a SOI term. However, the real practical interest of SHE as an approach of spin current generation in spintronics devices has appeared recently after the discovery of intrinsic SHE [19,20]. After this, two seminal experiments on the SHE have been done [22,23]. In this paper the SHE

is studied in a two-dimensional electron system undergoing Rashba SOI of both intrinsic and EP induced types, which are specific for GaN/AlGaN heterostructures, for example. Some new peculiarities of SHE, induced by interband interaction of heavy and light hole bands through electrical polarization or displacement like that of optical phonons are revealed in p-doped semiconductors with band degeneracy in the framework of Luttinger Hamiltonian.

2. Materials and structures for spin injection and detection in semiconductor Spintronics

The first approach for spin formation, injection and detection is based on using heterostructure with magnetic components. In the latter the carrier spin polarization appears in natural way due to the exchange interactions of the carriers with the material magnetic subsystem. The principles of injection as well as detection are simple and is sketched in Fig. 2.

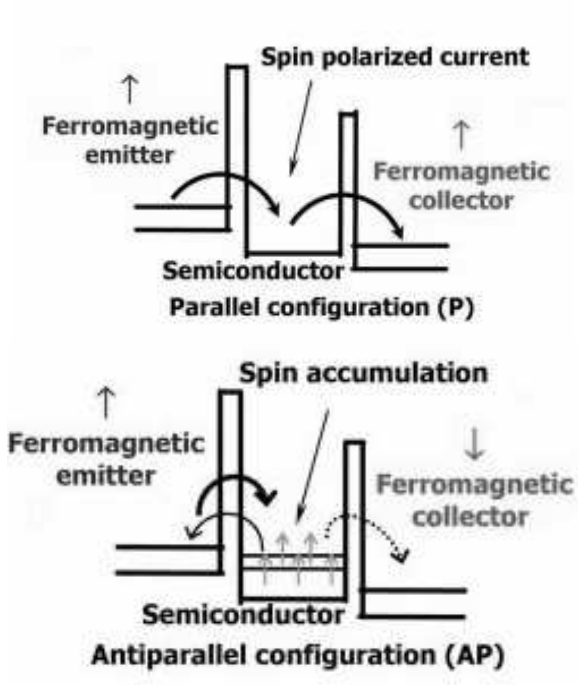

Fig. 2. Sketches illustrating spin injection (up) and spin detection (down).

Since spintronic injector devices are typically heterojunctions, it is important to have an efficient spin dependent transport across the interface between different materials with high degree of carrier spin polarization and the interfacial transparency. Efficient spin-polarised carrier injection at room temperature can be achieved following several routs. The first deals with carrier injection from ferromagnetic metals into a semiconductor. The material requirements for the integration of ferromagnetic metals and semiconductors are quite stringent. The ferromagnets must be: i) grown epitaxially on the semiconductors; (ii) thermodynamically stable with no interfacial reactions; and (iii) morphologically stable on the semiconductors. Among such hybrid structures have been found that the combination of MnAs metal and GaAs semiconductor is suitable enough. Although their crystal structures, lattice constants and chemical bonding natures are dissimilar, this combination has the following advantages:

1. All-epitaxial structures can be grown on commonly used semiconductor (GaAs and Si) substrates.
2. Thermodynamically stable heterointerfaces are obtained because MnAs and GaAs have common As atoms.
3. The growth process is completely compatible with the existing III–V MBE technology.
4. Not only single heterostructures, MnAs/III–V/MnAs trilayers for magnetic tunnel junctions, can be epitaxially grown on GaAs, as will be shown later.

A gate electrode may also be used on the semiconductor for additional control of spin and charge transport. Initial results with this approach proved disappointing, with low (~1%) injection efficiency [24]. A theoretical framework for these results was developed by Schmidt et al. [8], indicating that efficient injection was only obtainable in the diffusive regime when the conductivity of the injector material and the semiconductor was of similar magnitude or if the magnetic material is completely spin polarized (i.e., at the Fermi level, all carriers are of one spin state). Recent work has shown that this limitation may be circumvented using ballistic transport from tunnel barriers or Schottky contacts, for example [25]. For the case of Ni/GaAs, currents with >90% spin polarization in the GaAs were reported [26] and in device structures, high efficient spin-injection has been found for Fe/LED (light emitting diode) structures [27].

The second approach for realizing high spin injection efficiencies is to use magnetic semiconductors as a spin emitter, which can have completely, spin polarized carriers at the Fermi level. For this perspective class of spintronics materials it is important to underline the following advantages:

- Technological compatibility;
- Possibilities of ferromagnetic property tuning;
- Combination of magnetic and semiconductor properties;
- Spintronics multifunctionability

Significant progress has been made in manipulating spin dynamics in semiconductors, including various methods to create spin-polarized carriers, such as employing a novel class of ferromagnetic syastems and spin injection from a ferromagnet [28]. These advances, together with tunable electronic properties (such as carrier density and Fermi velocity) and well-established fabrication techniques, provide a compelling reason to study hybrid semiconductor structures in the context of spintronics [1].

Last years, research in diluted magnetic semiconductors (DMS) has been an area of great interest because they have a great potential for different spintronic tasks. In the context of spin injection and detection as well as for memory cells the ferromagnetic systems are more

important. Studies have been performed on various materials and structures, which can have a Curie temperature (T_c) above the room temperature, because the spintronics devices have eventually to be operated at room temperature. Among these materials, the III-V, II-VI and IV-VI DMS have attracted much attention during the early years of research. In particular the III-Mn-As DMS have been grown and confirmed to be ferromagnetic [29]. Important aspect of these DMS systems is its inherently compatible with existing GaAs technology, resulting in the practical realization of device structures combining ferromagnetic and nonmagnetic layers.

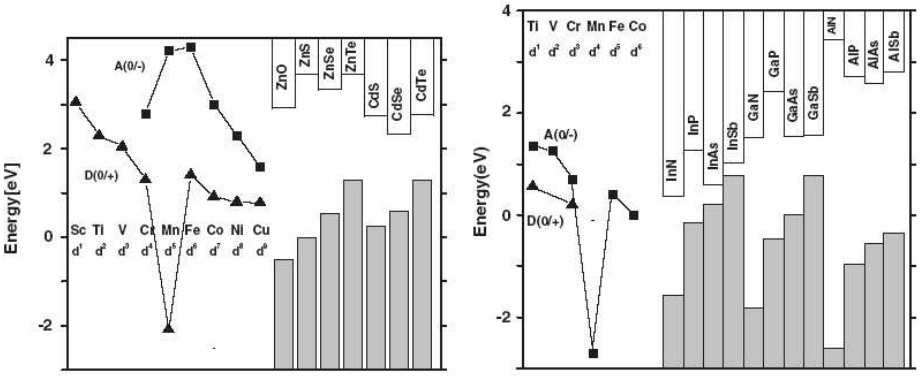

Fig. 3. Positions of transition metals levels relative to the conduction and valence band edges of II–VI (left panel) and III–V (right panel) compounds. By triangles the dN/dN−1 donor and by squares the dN/dN+1 acceptor states are denoted (adapted from [30]).

The evidence of Mn among others transition metal elements for DMS synthesis is a result of Mn impurity energy levels in the semiconductor compound hosts. Figure 3 illustrates the arrangement of transition metal levels relative to the band structure of the host semiconductors. A striking property of Mn is to have a deep emplacement of the impurity levels in the valence and conduction bands. In result ferromagnetic order in Mn-based DMS is mediated by carriers residing in relatively wide valence bands, while the d levels of other transition metals reside in the band gap of III–V and II–VI compounds and in such a situation the double exchange may constitute the dominant mechanism of spin–spin interactions.

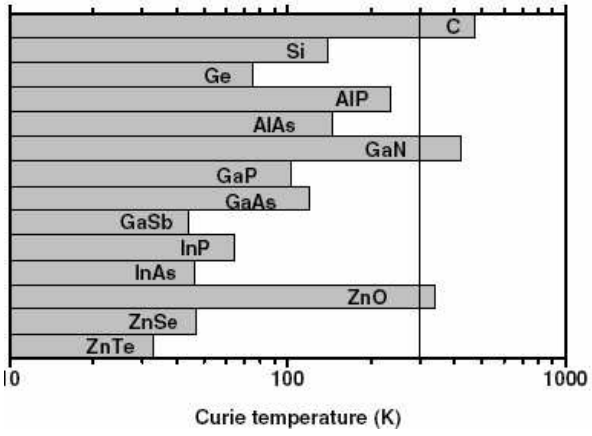

Fig. 4. Computed values of the Curie temperature T_c for various p - type semiconductors containing 5% of Mn per/cation (2.5% per/atom) [10].

It is well established that Mn is divalent in II–VI compounds, and assumes the high spin d5 configuration characterized by $S = 5/2$ and $g = 2.0$. The spin dependent hybridization between anion p and Mn d states leads to the superexchange, a short-range antiferromagnetic coupling among the Mn moments, and MnAs or MnTe compounds, for example, are antiferomagnetic. However, it is important that antiferromagnetic superexchange can be overcompensated by ferromagnetic interactions mediated by band holes in DMS. In the result DMS can become ferromagnetic with magnetic properties tailored by carrier concentration.

For III–V compounds it is established that the Mn acts as an effective mass acceptor (d5+h) in the case of antimonides and arsenides. The ESR measurements of GaAs:Mn show, in addition to the well known spectrum of Mn d^5 with the Lande factor $g_{Mn} = 2.0$, two additional lines corresponding to $g_1 = 2.8$ and $g_2 \approx 6$ [31], which can be described quantitatively within the $k \cdot p$ scheme for the occupied acceptor. In these III–V materials, one hole localized at two Mn ions generates, via Zener's double exchange, a strong ferromagnetic coupling that overcompensates the intrinsic superexchange antiferromagnetic interaction of Mn ions. At the same time, in II–VI compounds acceptor cores do not carry any spin and the degree of compensation by donors is low. In comparison to antimonides and arsenides, the situation is another in the case of phosphides and nitrides. Their ESR spectra show only the presence of a line with $g = 2.0$ [33], which is thus assigned to d^5 centres. This, together with the lack of manifestation for d5+h states, even in p-type materials, appear to indicate on Mn in the ground state of the d^4 shell electron configuration not d^{5+h} [32]. In this case, the spin–spin interaction seems to be driven by a double exchange mechanism involving hopping of d-electrons [33], as in the case of colossal magnetoresistance manganites, not by the holes in the valence band. Thus despite much common properties in III–V DMS compounds there are peculiarities of the interference of magnetic and semiconductor features.

The existing data (Fig. 4) illustrate that there is much room for a further increase of T_c in p-type DMS. In particular, a general tendency for greater T_c values in the case of lighter elements stems from the corresponding increase in p–d hybridization and the reduction of the spin–orbit coupling. Thus in this class of materials improving the functionality for spin injection based on good magnetic properties, while the functionality for spin manipulation provided by sufficient SOI coupling is reducing.

Recently, for the past couple of years, great interest has been focused on DMS based on GaN, because gallium nitride is undoubtedly one of the most promising materials for application in electronic and optoelectronic devices like GaAs and a theoretical calculation predicted that DMS based on GaN doped with Mn would have a Tc above 300 K (Fig.4). A number of different methods for introducing Mn into GaN have proven successful in producing ferromagnetism. For example, in epitaxial GaN layers grown on sapphire substrates and then subjected to solid state diffusion of Mn at temperatures from 250-800 °C for various periods, clear signatures of room temperature ferromagnetism were observed [34]. The Curie temperature was found to be in the range 220-370 K, depending on the diffusion conditions. In (Ga,Mn)N films grown by MBE at temperatures between 580-720 °C with Mn contents of 6-9 at.%, magnetization (M) versus magnetic field (H) curves showed clear hysteresis at 300 K, with coercivities of 52-85 Oe and residual magnetizations of 0.08-0.77 emu/g at this temperature [35].

Past reviews have covered concentrated magnetic semiconductors such as Eu chalcogenides [36], all of which have T_C's<150 K and mixed-valence perovskites [37]. Much progress has also been made in half-metallic CrO_2, which displays a T_C of 400K and a magnetic moment of 2 μ_B per Cr atom[38],Fe_3O_4,which is a hopping conductor ferromagnet with a T_C of 865 K [39], Heusler alloys such as Ni_2MnGa [40], Ni_2MnIn [41] and Ni_2MnSb[42]], the latter with a T_C of 728 K and finally, metastable CrAs [43]], which are room temperature ferromagnets. Half metallic materials such as the Heusler alloys are also of interest in application to metallic spin-valves and magnetic tunnel junctions (currently deployed in magnetic hard disk drive read heads and non-volatile elements in the magnetic random access memory (MRAM) applications).

Selection of the most promising spin injection materials for semiconductor spintronics is based on two main criteria. First, the ferromagnetic state of the materials should be preserved at temperatures higher than 300 K. Second, there is significant advantage if the technology base for such material already exists in other applications. Most of the work in the past has focused on (Ga,Mn)As and (In,Mn)As. There are indeed major markets for their host materials in infra-red light-emitting diodes and lasers and high speed digital electronics (GaAs) and magnetic sensors (InAs). However, the highest Curie temperatures reported for these materials (~110 K for (Ga,Mn)As and ~35 for (In,Mn)As are yet too low for most practical applications.

In the search for model high quality semiconductor magnetic structures that would allow for the practical demonstration of anticipated new spintronic and spin-optoelectronic functionalities, new group of semiconductor spintronic structures is developed and investigated, namely, the all-semiconductor magnetic-nonmagnetic multilayers on the basis of IV-VI semiconductors and europium chalcogenides. They are built of very well lattice-matched materials which can be epitaxially grown in a controlled way to achieve very high structural and electronic quality of both magnetic and nonmagnetic layers. Semiconductor magnetic multilayer structures composed of nonmagnetic layers of IV-VI semiconductors (e.g PbS or PbTe) and ferromagnetic (EuS) or antiferromagnetic (EuTe) layers have been fabricated [44]. All these compound semiconductors crystallize in rock salt structure with a number of well lattice-matched pairs of materials. The ferromagnetic-nonmagnetic EuS-PbS heterostructure (with lattice parameters of PbS and EuS differing only by 0.5%) is particularly important. EuS is a model nonmetallic Heisenberg ferromagnet whereas PbS is the narrow energy gap IV-VI semiconductor compound well known for its infrared optoelectronic properties.

The electronic structure of EuS-PbS multilayers can be as multiple quantum well of nonmagnetic PbS with ferromagnetic (below 16.6 K) barriers of EuS. Due to ferromagnetic character of EuS the height of the electron barrier bounding electrons in PbS quantum wells depends on the magnetization of EuS layers and strongly differs for electrons with opposite spin directions. While tunneling through EuS barrier electrons are strongly spin filtered (i.e. transmission coefficient for electrons with one spin direction is much larger than that for electrons with opposite spin direction). In EuS-PbS-EuS tunneling structures with double ferromagnetic barrier it is expected to allow for very efficient control of spin dependent flow of current resulting in large tunnelling magneto-resistance (TMR) – one of spintronics functions envisioned. The exceptional effectiveness and robustness of EuS as ferromagnetic spin filter material was already experimentally demonstrated in heterostructures with metals [45]. A new dimension in the control of such structures is provided by recently discovered effect of interlayer coupling that is responsible for an antiferromagnetic alignment of magnetization vectors of neighboring EuS layers at zero fields with a possibility to switch between antiferromagnetic and ferromagnetic arrangement using low external magnetic fields. It offers a unique scenario for magnetic field control of all-semiconductor magnetic tunnelling junctions [45]. In photo-luminescent as well as electrical bipolar structures with EuS double ferromagnetic barriers the electrons and holes injected into the optically active PbS quantum well posses a selected (spin filtered) spin direction. Recombining radiatively, they produce specific (magnetization controlled) polarization of light emitted from such a structure as recently demonstrated in diluted magnetic semiconductor structures [7, 8, 9]. The type-I arrangement of the conduction and valence band edges at the EuS-PbS heterointerface and a direct energy gap of

PbS assures that both electrons and holes (doped, photo-generated or electrically injected) occupy the electronic states in the PbS quantum well. This is the electronic band structure optimal for making mid-infrared light emitting diodes and lasers. The presence of ferromagnetic electron barriers is expected to allow for the temperature and magnetic field fine tuning of the radiation wavelength generated or detected in these structures as well as the control of the polarization state of this radiation. Recently, the high technological opto-electronic perfection was experimentally demonstrated for the closely related EuTe-PbTe/BaF_2 multilayers of which the optically pumped vertical-cavity surface-emitting laser structures were fabricated [46].

EuS abd EuTe layers with Gd offer a new exciting possibility to use EuGdS and EuGdTe as fully spin polarized electronic injectors. This property of these materials stems from the large exchange splitting of the conduction band states observed below the Curie temperature [47]. It is expected that these materials may serve as injectors in spintronic structures built of both IV-VI (PbS, PbTe) and II-VI (CdTe) semiconductors. Another advantage in this field can be the use of complex buffer layers which allow for the epitaxial matching of Si substrates and IV-VI semiconductors – a technological approach which offers the possibility of spintronics integration with traditional microelectronics [48]. In Table 1 a summary of the parameters of the high-temperature ferromagnetic semiconductors is presented.

Table 1. Summary of semiconductors exhibiting room temperature ferromagnetism.

Material	Bandgap (eV)	Synthesis	T_C(K)
$Cd_{1-x}Mn_xGeP_2$	1.72	Solid-phase reaction of evap. Mn	>300
(Ga,Mn)N	3.4	Mn incorporated by diff^n	228-370
(Ga,Mn)N	3.4	Mn incorporated during MBE; n-type	>300
(Ga,Mn)N	3.4	Mn incorporated during MBE	940
(Ga,Cr)N (Ga,Cr)N	3.4 3.4	Cr incorporated during MBE Bulk growth	>400 >300K
(Ga,Mn)P:C	2.2	Mn incorporated by implant or MBE; p ~10^{20} cm^{-3}	>330
$(Zn_{1-x}Mn_x)GeP_2$	1.83-2.8	Sealed ampule growth; insulating; 5.6% Mn	312
$(ZnMn)GeP_2$	< 2.8	Mn incorporated by diff.	350K
$ZnSnAs_2$	0.65	Bridgman bulk growth	329K
$ZnSiGeN_2$	3.52	Mn-implanted epi	~300

The third method of efficient spin injection is related to the digital structures and so-called spin filtering tunnelling structures.

In order to realize spintronics devices in digital alloys, recent studies have been carried out on the well-known InAs/GaSb-based materials and structures [49]. As a key component to such devices, GaSb/Mn digital alloys were successfully grown by molecular beam epitaxy. Good crystal quality was observed with transmission electron microscopy showing well-resolved Mn-containing layers and no evidence of 3D MnSb precipitates in as-grown samples. Ferromagnetism was observed in GaSb/Mn digital alloys with temperature-dependent hysteresis loops in magnetization up to 400 K (limited by the experimental setup). One key advantage of semiconductors for electronic spintronic applications is the relative ease with which carrier density can be modified by either applied electric bias or photoexcitation. Although there has been an attempt to control ferromagnetism in (Ga,Mn)As and (Al,Ga,Mn)As by electric field, the experimental results showed that there was no observable electric field modulation of T_C or of the magnetization in these materials. The effect of applied electric bias on ferromagnetism was demonstrated recently for GaSb/Mn digital alloys.

A lot of different tunnelling structures have been proposed to create spin-polarized current. Among them it is worth to underline the all-semiconductor structures based on SOI mechanism of spin-faltering. The most exploring was the Rashba SOI mechanism [50]. However, spin-polarized tunnel characteristics appear only in asymmetric barrier structure due to the difference in the values of the effective masses in the barrier leads. Therefore the rate of spin-polarization is very low. Some proposals to enhance the rate of polarization deal with resonant tunneling structures [51].

In a single symmetric barrier structure spin-polarized tunneling it was suggested to get in a layered structure

with dominant Dresselhaus SOI interaction [52]. The energetic diagram and the calculated tunnel characteristics are reproduced in Fig. 5.

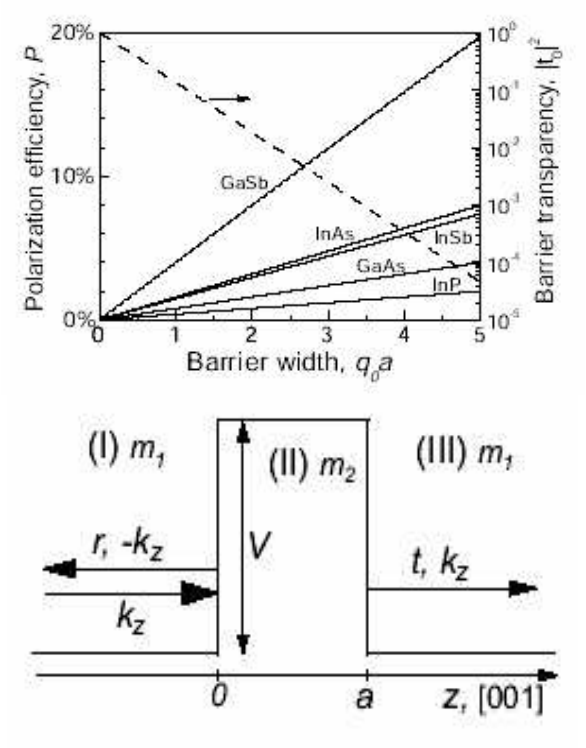

Fig. 5. Energy diagram of symmetric barrier structure (up) and calculated tunnel parameters for different structures with Dresselhaus SOI interaction (down)[52].

Another variant or formation of spin-dependent tunneling transport in a symmetric barrier structures has been proposed by us [11,18] on the basis of SOI induced by electrical polarization. The tunneling characteristics of such structure are presented in Fig. 6 and 7.

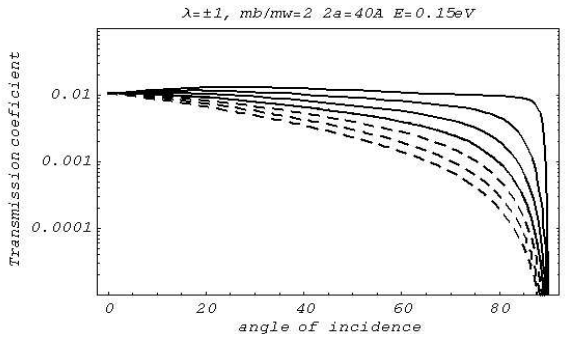

Fig. 6. Variation of the transmission coefficient via angle of incidence of electron beam for barrier structure with height V_0 = 300 meV and width 2a = 40 A. Curves A, B, C and D are plotted for incident energy E = 450, 350, 250, 150 meV respectively. Dotted lines are for spin down and solid lines for spin up.

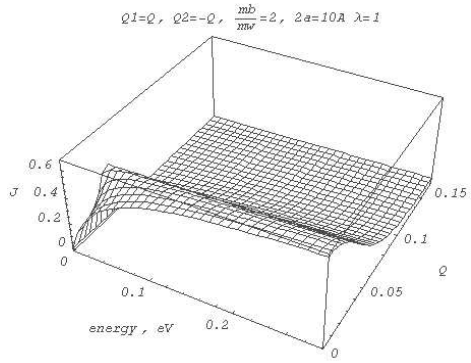

Fig. 7. Tunneling current of spin-up carriers in dependence of their energy and dimensionless parameter of electrical polarization of the barrier structure.

A new approach to create systems with spin-polarization for injection was proposed on the basis of stressed semiconductor heterojunctions with anti-ferromagnetic ordering, in which the constituents have opposite band-edge symmetry and their gaps have opposite signs [53]. Interface states have been shown to appear in these heterojunctions, and they are spin split. If the Fermi level lies in one of the interface bands, this results in magnetic ordering in the interface plane. The interface magnetization effect is expected to take place.

3. Methods and structures for spin manipulation and for testing spin parameters of carriers

The emerging field of spintronics has focused primarily on issues of spin injection and detection in semiconductor systems and magnetoresistance and related phenomena in inhomogeneous metallic systems. In semiconductors with large spin–orbit splittings the coupling of spin polarization with electric fields or currents offers new opportunities for spin manipulation in both electronic and optoelectronic devices.

SOI is considered to be the main channel for spin manipulation due to:

i) comparatively large magnitude;

ii) possibilities of using electric fields and optical phenomena for modification of spin states.

The methods of effective control and manipulation of the spin system through SOI mechanisms in semiconductor spintronics can be divided in three categories:

- Optical
- Electrical
- Magnetic

A variety of optical methods and techniques are employed to investigate spin-dependent effects in semiconductors and quantum structures [54]. Time-resolved Faraday rotation (TRFR) is a versatile optical technique that enables the study of environmental contributions to electron-spin decoherence in a variety of semiconductors [55]. Usually the spin of the holes relaxes relatively quickly (<1 ps), and this provides to analyze the evolution of electron spins. In Fig. 8 the sketch of TRFR method of investigation is reproduced [54].

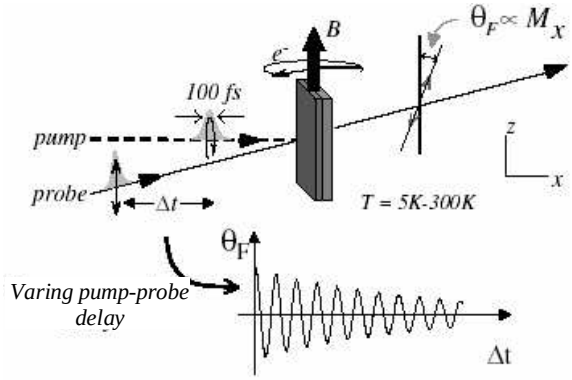

Fig. 8. Experimental geometry for time-resolved Faraday rotation (TRFR) [54].

Laser systems are used to produce ~100 fs pump and probe pulses that are broadly tunable in the near-infrared and blue regions of the spectrum. An optical parametric amplifier is employed as a source of pulses tunnable across the visible (500–700 nm). A non-equilibrium transverse spin polarization is excited by a circularly polarized pump pulse in correspondence with optical selection rules. In the presence of a perpendicular magnetic field B, the pump-excited spins comprise a coherent superposition of spin eigenstates quantized along the magnetic field direction. The temporal evolution of this superposition corresponds to Larmor spin precession at the frequency: $h\nu_L = g_e\mu_B B$, where g_e is the electron g-factor. The component of spin magnetization along the laser direction creates a transient circular birefringence that is recorded as the Faraday (Kerr) rotation of a time-delayed, linearly polarized probe pulse which passes through (or is reflected from) the sample. Measurement of the time delay between the pump and probe allows one to directly monitor spin precession in the time domain.

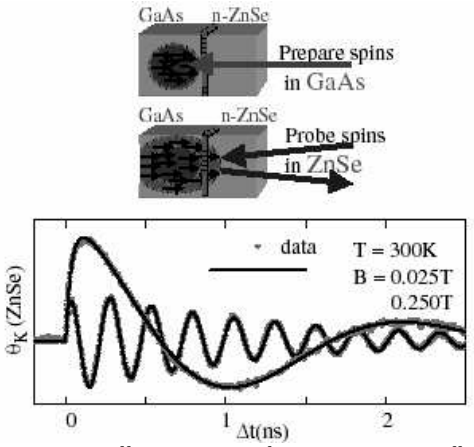

Fig. 9. Tow - collar pump – probe measurements allow one to study the diffusion of coherent spin across a heterointerface. TRFR in GaAs/ZnSe at T = 300 K [56].

In order to investigate the electrical transport of spin coherence across semiconductor heterojunctions, a two-colour pump–probe technique has been developed in which the excitation and measurement of spin occur in different layers [56]. This is made possible by actively synchronizing two laser sources to produce pump and probe pulses, their energies can be independently tuned. Fig9 shows that spin coherence can be transferred from GaAs to ZnSe, two semiconductors with radically different bandgaps (~1.5 eV versus 2.8 eV) and electron g-factors (-0.44 versus 1.1). Here electron spin is initially excited in the GaAs substrate, and allowed to diffuse into the ZnSe epilayer. Once the electron spin crosses into the ZnSe, it precesses in accordance with the ZnSe g-factor and spin lifetime. Because the spin lifetime in the undoped GaAs substrate is short (~100 ps), these data show that one can preserve spin coherence by transferring to regions with intrinsically lower decoherence. In both these shortly described methods semiconductor materials with good Faraday angle rotation have been used. Also it is important to note the robustness of the spin degree of freedom in semiconductors, which is evidenced by the fact that this process works at room temperature [56].

The question of how spins of mobile electrons (and holes) lose their spin coherence is thus of the utmost importance for spintronic technology and for solid-state quantum computing. Unfortunately, the physical picture of spin decoherence (or relaxation) is now far from complete. Most information comes from experiments, but experimental data are still scarce and often incomplete. Spin relaxation rate $1/T_1$ increases as temperature increases, with the growth becoming linear above the Debye temperature. The Elliott- Yafet mechanism is the most important spin relaxation mechanism in metals and semiconductors with inversion symmetry. It gives typical values of T_1 on the nanosecond scale, in agreement with experiment. The situation is much more complicated in semiconductors [57]. Many interesting semiconductors like GaAs lack inversion symmetry, so that other mechanisms, in addition to the Elliott-Yafet one, become important [57]. These mechanisms operate differently in different temperature regions, doping, and magnetic, strain, and confinement fields, so that sorting out the relevant mechanism(s) for a given material is a tremendous task which is yet to be carried out. Magnitudes of T_1 in semiconductors are also typically nanoseconds, but recent experimental studies in II-VI and III-V systems show that T_1 can be artificially enhanced [57].

Wave function and spin engineering as well as electrical gating in semiconductor heterostructures including materials with different *g*-factors is employed to control coherent electron-spin precession [58]. An Al*x*Ga1–*x*As quantum well with parabolically graded Al concentration is specially designed for this purpose. In such way the electron *g*-factor can be tuned while displacing the electron wave function with electrical bias by using the variation in *g*e with Al concentration *x* (in bulk Al*x*Ga1–*x*As, *g*e = –0.44 for *x* = 0 and *g*e = 0.40 for *x* = 0.3) . While the parabolic shape of the potential does not change with application of an electric field, the minimum can be displaced to a region with higher Al content. This allows the displacement of the whole electron wave function without distortion in contrast to a square quantum well, where only the tail of the wavefunction is pushed into the barrier. Time-resolved Kerr rotation (TRKR) probes the electronspin dynamics, demonstrating gate-voltage mediated control of coherent spin precession.

4. Spin hall effect in spintronics functinability

Among promising variants of spin injection during last years spin Hall effect (SHE) is considered, which in its extrinsic form has been discovered more than two decades ago [21]. The extrinsic SHE is related to skew-scattering mechanism [21] and is based on asymmetric scattering of spin-up and spin-down electrons from a random impurity potential that includes a SOI term. However, the real practical interest to this approach of spin current generation has appearing recently after the discovery of intrinsic SHE [19,20], when Murakami, Nagaosa, and Zhang [19] proposed it in hole doped semiconductors like p-GaAs, and Sinova et al. [20] proposed the SHE in n-type two-dimensional semiconductor heterostructures. After this, two seminal experiments on the SHE have been done. Kato et al. [22] observed spin accumulation in n-type GaAs by means of Kerr rotation, and Wunderlich et al. [23] observed a circularly polarized light emitted from a light-emitting diode (LED) structure, confirming the SHE in p-type semiconductor.

The geometrical structure of the intrinsic SHE is such that for an electric field applied, for example, on the z direction, a y-polarized dissipationless spin current will flow in the x direction (Fig. 10). The electric field induced spin current can be summarized by the following macroscopic relation

$$J_j^i = \sigma_s \varepsilon_{ijk} E_k \qquad (4.1)$$

where σ_S is the spin conductance, ε_{ijk} is antisymmetric tensor.

At the same time, at the microscopic level the spin current is defined as the produce of velocity and the spin and is a rank two tensor. However, the velocity operator in general does not commute with the spin operator in a model with spin-orbit coupling. In order to define the spin current tensor as Hermitian operator it is symmetrized as:

$$J_j^i = \frac{1}{2}\left(S_i \frac{\partial H}{\partial P_j} + \frac{\partial H}{\partial P_j} S_i \right) \qquad (4.2)$$

where S_i is the projection of the spin.

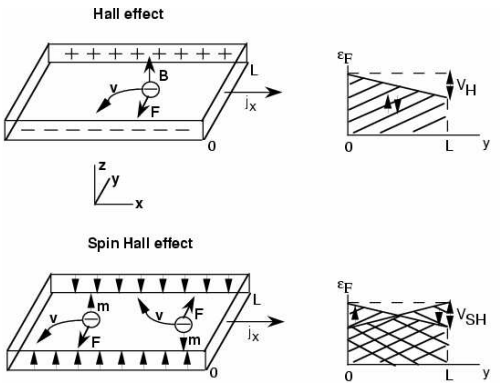

Fig. 10. Schematic illustration of the traditional Hall effect (up) and spin Hall effect geometries (down) with the evolution of Fermi level.

The induced spin current is considered to be dissipationless and unlike the anomalous Hall Effect can be realized even in non-magnetic systems. Murakami et al. [19] and Sinova et al. [20] have argued, in contexts of p-doped semiconductors and 2D Rashba coupled systems, that spin-Hall conductivity can be dominated by an intrinsic contribution that follows from distortion of Bloch electrons by the electric field and therefore approaches a disorder independent value in high mobility systems. The aspect of dissipationless is one of the central issues of SHE both from fundamental and practical points of view.

In the first papers the analysis of intrinsic SHE was done on the basis of semiclassical approach. In two-dimensional n-type systems, studied in [19], the Hall conductivity σ_{xy} in a clean limit is calculated from the Kubo formula as

$$\sigma_{xy} = -\frac{e^2}{2\pi\hbar} \sum_n \int_{BZ} d^2\vec{k}\, n_F\left(\varepsilon_n\left(\vec{k}\right)\right) B_{nz}\left(\vec{k}\right), \qquad (4.3)$$

where n is the band index, and integral is over the entire Brillouin zone. $B_{nz}\left(\vec{k}\right)$ is defined as a z component of $\vec{B}_n\left(\vec{k}\right) = \nabla_{\vec{k}} \vec{A}_n\left(\vec{k}\right)$, where

$$\vec{A}_n\left(\vec{k}\right) = -i\left\langle nk\left|\frac{\partial}{\partial k_i}\right|nk\right\rangle \equiv -i\int_{\text{unit cell}} u_{nk}^{+} \frac{\partial u_{nk}}{\partial k_i} d^2x \qquad (4.4)$$

and u_{nk} is the periodic part of the Bloch wave function $\phi_{nk}(x) = e^{ikx} u_{nk}(x)$. This $B_{nz}\left(\vec{k}\right)$ represents the effect of Berry phase momentum space. $n_F\left(\varepsilon_n\left(\vec{k}\right)\right)$ is the Fermi distribution function for the n-th band.

By incorporating the effect of $B(k)$, the Boltzman-type semiclassical equation of motion acquires an additional term [59]:

$$\dot{x} = \frac{1}{\hbar}\frac{\partial E_n(k)}{\partial k} + \dot{k} \times B_n(k)$$
$$\hbar\dot{k} = -e\left(E + \dot{x} \times B(x)\right) \qquad (4.5)$$

The term $\dot{x} \times B(x)$ represents the effect of Berry phase, and it is called anomalous velocity. Under the external electric field, the anomalous velocity becomes perpendicular to the field, and gives rise to the Hall effect. This Hall current is distinct from the usual Ohmic current, which comes from the shift of the Fermi surface from its equilibrium. This Hall effect comes from all the occupied states, not only from the states on the Fermi level. Sinova et al. [20] applied the Kubo formula to this Rashba Hamiltonian

$$H_R = \alpha_R\left(\sigma_x \hat{k}_y - \sigma_y \hat{k}_x\right) \qquad (4.6)$$

For this procedure, they defined the spin current J_{zy} to be a symmetrized product of the spin Sz and the velocity

$$v_y = \frac{\partial H}{\partial k_y}. \qquad (4.7)$$

By assuming no disorder, the resulting spin Hall conductivity

$$\sigma_{sH} = \frac{-e}{16\pi\lambda m}\left(p_{F+} - p_{F-}\right) \qquad (4.8)$$

where p_{F+} and p_{F-} are the Fermi momenta of the majority and minority spin Rashba bands. However, when $n_{2D} > m^2\lambda^2/\pi\hbar^4 \equiv n_{2D}^*$, $p_{F+} - p_{F-} = 2m\lambda/\hbar$ and the spin Hall conductivity is

$$\sigma_{sH} = -\frac{j_{s,y}}{E_z} = \frac{e}{8\pi} \qquad (4.9)$$

independent of both the Rashba coupling strength and the 2DES density.

The origin of the SHE in this model is the following. The Rashba term (4.6) can be regarded as a k- dependent effective Zeeman field $B_{eff} = \alpha(z \times k)$. In equilibrium the spins are pointing either parallel or antiparallel to B_{eff} for the lower and upper bands, respectively. An external electric field $E \| x$ changes the wave vectors k of Bloch wave functions, and B_{eff} also changes accordingly. The spins will then precess around B_{eff}, and tilt to the $\pm z$-direction, depending on the sign of k_y. This appears as the SHE, and the spin Hall conductivity is calculated to be $\frac{e}{8\pi}$, in agreement with the Kubo formula.

The Dresselhaus term

$$H_D = \alpha_D\left(\sigma_x \hat{k}_x - \sigma_y \hat{k}_y\right) \qquad (4.10)$$

can also be incorporated and if this SOI is stronger than Rashba ones spin Hall conductivity changes the sign.

By straightforward calculation following [20] it is easy to incorporate the influence of Rashba like SOI induced by electrical polarization, oriented normal to the 2D systems. As follows from the analysis [18] in this case the electrical induced SOI leads only to renormalization of Rashba constant.

In general case both Rashba and Dresselhaus like terms generated by electrical polarization appear, and their effect is similar to established effect of intrinsic ones.

Initially the intrinsic SHE in p-type systems have been studied [19] in bulk semiconductors on the basis of isotropic effective Luttinger Hamiltonian of the two-fold degenerate valence bands of conventional semiconductors such as Si, Ge, GaAs, etc.

$$H_L = \frac{1}{2m}\left[\left(\gamma_1 + \frac{5}{2}\gamma_2\right)P^2 - 2\gamma_2 (PS)^2\right], \qquad (4.11)$$

where $S = (S_x, S_y, S_z)$ are spin 3/2 matrices, γ_1 and γ_2 are the Luttinger constants.

Following [60] in semiclassical approximation is straightforward to get the relation for spin Hall conductivity. The semiclassical equations of motion for holes under an electric field E read as

$$\dot{x} = \frac{1}{\hbar}\frac{\partial E_\lambda(k)}{\partial k} + \dot{k} \times B_\lambda(k) \quad \hbar\dot{k} = -eE \qquad (4.12)$$

Here $E_\lambda(k) = \frac{\hbar^2 k^2}{2m}\left(\gamma_1 + \left(5/2 - 2\lambda^2\right)\gamma_2\right)$ is an eigenenergy for the band with helicity λ. The Berry curvature is given by $B_\lambda(k) = \lambda\left(2\lambda^2 - 7/2\right)\vec{k}/k^3$, which depends on the helicity.

If there is no anomalous velocity, the holes will move parallel to $\vec{k}$. The Berry curvature gives rise to an anomalous velocity perpendicular to both $\vec{k}$ and $\vec{E}$. This anomalous velocity is opposite for opposite helicity, i.e. for opposite spin orientation. This anomalous velocity from the motion along $\vec{k}$, when summed over all $\vec{k}$ of occupied states, amounts to a spin current. In the zero temperature, by applying an electric field along the l-direction, the spin current in which spins along the i-axis will flow along the j-direction is calculated as

$$j_j^i = \frac{e}{12\pi^2}\left(3k_F^H - k_F^L\right)\varepsilon_{ijl}E_l \qquad (4.13)$$

Here, k_F^H and k_F^L are the Fermi wavenumbers for the HH and the LH bands, respectively.

A schematic of this effect is shown in Fig. 11 (a).

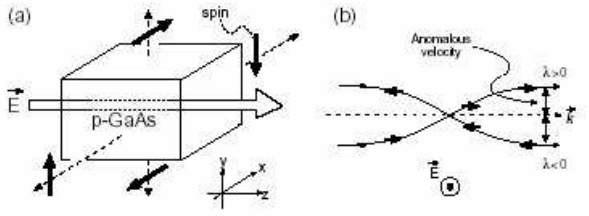

Fig. 11 (a). Schematic of the spin Hall effect for p-type semiconductors [54]. (b) Semiclassical trajectories for the wavepackets with helicity λ, projected onto the plane perpendicular to the electric field E. The thick arrows represent the spins.

Taking into account the interband interaction through optical phonons [61] the SOI induced by electrical polarization or optical like displacement can be incorporated into effective Luttinger Hamiltonian in the following form:

$$\begin{pmatrix} 0 & iu_y+u_x & -iu_z & 0 \\ -iu_y+u_x & 0 & 0 & -iu_z \\ iu_z & 0 & 0 & -iu_y-u_x \\ 0 & iu_z & iu_y-u_x & 0 \end{pmatrix} \quad (4.14)$$

Thus the generalized effective Luttinger Hamiltonian including both induced SOI and the anisotropy terms of the holes is written as

$$\hat{H}=\frac{\hbar^2}{2m^*}\left[\left(\gamma_1+\frac{5}{2}\gamma_2\right)k^2-2\gamma_2\left(k_x^2S_x^2+k_y^2S_y^2+k_z^2S_z^2\right)-\right. \quad (4.15)$$
$$\left.-4\gamma_3\left(\{k_x,k_y+u_z\}\{S_x,S_y\}+\{k_y,k_z+u_x\}\{S_y,S_z\}+\{k_z,k_x+u_y\}\{S_z,S_x\}\right)\right]$$

where $\left[S_i,S_j\right]=\frac{1}{2}\left(S_iS_j+S_jS_i\right)$.

Taking into account that Luttinger like Hamiltonian (1) has two eigenvalues of light and heavy hole states following the recently proposed approach [62] terms in the anisotropic Luttinger Hamiltonian can be transformed in terms of a Clifford algebra of Dirac Γ matrices $\{\Gamma_a,\Gamma_b\}=a\delta_{ab}I_{4x4}$ $\hat{H}=\gamma_1k^2+2\gamma_3d_a\Gamma_a$

Where

$$d_1=-\sqrt{3}k_zk_y+\sqrt{3}u_x,$$

$$d_2=-\sqrt{3}k_zk_x+\sqrt{3}u_y, d_3=-\sqrt{3}k_xk_y+\sqrt{3}u_z$$

$$d_4=-\frac{\sqrt{3}}{2}\frac{\gamma_2}{\gamma_3}\left(k_x^2-k_y^2\right), d_5=-\frac{1}{2}\frac{\gamma_2}{\gamma_3}\left(2k_z^2-k_x^2-k_y^2\right)$$

and $\frac{\hbar^2}{2m^*}\gamma_j\to\gamma_j$.

The eigenvalue of the operator $d_a\Gamma/d$, where $d^2=d_ad_a$ are ±1 so that, the eigenvalues of $\hat{H}$ are:

$$E(k)=\gamma_1k^2\pm2\gamma_3d(k)$$

where

$$d^2(k)=\left(\frac{\gamma_2}{\gamma_3}\right)^2k^4+3\left(1-\left(\frac{\gamma_2}{\gamma1}\right)^2\right)\left(k_x^2k_y^2+k_y^2k_z^2+k_z^2k_x^2\right)+$$
$$+3u^2+6\left(k_xk_yu_z-k_yk_zu_x-k_zk_xu_y\right)$$

The terms with polarization SOI lead to the spin splitting of heavy and light holes as illustrated in Fig. 12.

Following the approach [62] in spherical approximation and keeping only terms linear in u_j we obtain in analytical form the expression for spin conductance:

$$\sigma_{ij}^l=\sigma_{ij}^l0)+\sigma_{ij}^l(u)=\frac{1}{6\pi^2}\varepsilon_{ijl}\left(k_F^H-k_F^L\right)+\frac{1}{6\pi^2}\varepsilon_{ijl}u_l\left(\frac{1}{k_F^L}-\frac{1}{k_F^H}\right) \quad (4.16)$$

where k_F^H и k_F^L are the Fermi wave vector of heavy and light holes of bulk semiconductors respectively, ε_{ijl} is the antisymmetric tensor.

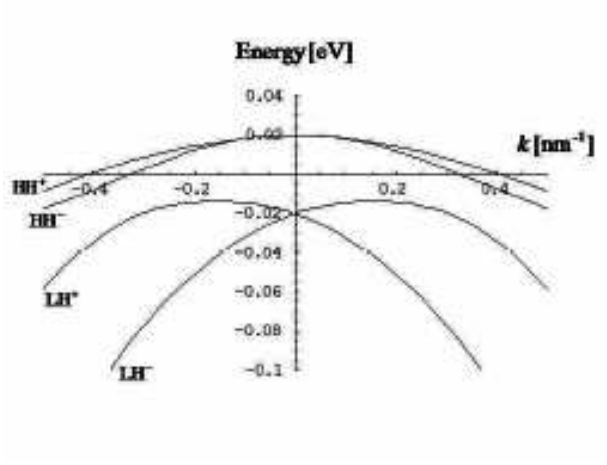

Fig. 12. Band splitting.by optical phonon like interband coupling in hole semiconductors.

The obtained formula (4.16) for spin-conductivity shows that the part $\sigma_{ij}^l(u)$ of conductivity induced by the polarization u in comparison with intrinsic part $\sigma_{ij}^l(0)$, considered in [19] is proportional to difference of the inverse values of the hole wave vectors. In result $\sigma_{ij}^l(u)$ for low doped semiconductors can exceed $\sigma_{ij}^l(0)$. $\sigma_{ij}^l(0)$.

The induced spin currents in the SHE are considered to be dissipationless. Murakami et al. [19] in the first paper have argued, that spin- the electric field and therefore approaches a disorder independent value in high mobility systems. The aspect of dissipationless is one of the central issues of SHE as well as recently proposed orbital angular momentum Hall effect (OAHE) from both fundamental and practical points of view. Although first papers [19,20], dedicated to the topics of intrinsic SHE, have appeared just at the same time, the proposed mechanisms of SHE are of different nature as follows from the above short analysis. In the Luttinger spin orbit coupling systems, a beautiful physical interpretation of the nature of intrinsic SHE was done. The origin of the spin- current comes from the existence of a monopole structure in momentum space, which are directly derived from the Berry phase in spin orbit coupling systems when Hamiltonian is projected to double degenerated helicity bands. Due to this topological nature, the conserved spin Hall current in general can be called as topological spin Hall current.

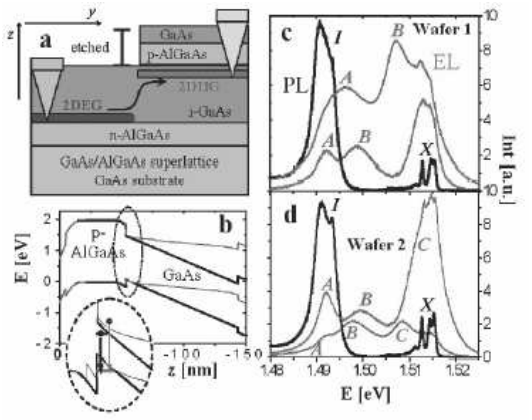

Fig. 13 (a). The schematic cross section of the coplanar p-n junction LED device. (b) Numerical simulations of the conduction and valence band profiles along the h001i growth direction (z axis) in the unetched part of the wafer near the step edge. Black lines correspond to an unbiased p-n junction and red lines to forward bias of 1.5 V across the junction. In the detailed image of the upper (AlGa)As/GaAs interface (with the conduction band shifted down in energy for clarity), it is indicated possible sub-GaAs-gap radiative recombinations with the 2DHG involving either 3D electrons in the conduction band (red arrow) or impurity states (black arrow). The black line corresponds to unbiased wafer 1 and the blue line to wafer 2. (c), (d) Photoluminescence spectra (black lines) and electroluminescence spectra (red lines) at low (lower curves) and high (higher curves) bias measured in wafers 1 and 2 at 4.2 K.

Experimentally, the SHE has been until recently elusive because in nonmagnetic systems the transverse spin currents do not lead to net charge imbalance across the sample, precluding the simple electrical measurement. In order to demonstrate the SHE and its new functionality in semiconductor spintronics, recently [23] a novel p-n junction light-emitting diode (LED) microdevice has been fabricated, in a similar spirit to the one proposed in [22]. The LEDs were fabricated in (Al,Ga)As/GaAs heterostructures grown by molecular-beam epitaxy and using modulation of donor (Si) and acceptor (Be) doping (Al,Ga)As barrier materials. The planar device features were prepared by optical and electron-beam lithography.

The sketch of LED structure and the results of both photo- and electroluminescence spectra are reproduced in Fig. 13.

In the LED structure forward bias of order of the GaAs band gap, electrons move from the 2DEG to the 2DHG where they recombine. The highest intensity of the emitted light is in the p region near the junction step edge. The numerical simulations of the band profile indicates the formation of the well both for electrons and holes. In measurements of photo- and electroluminescence spectra (Fig. 13 c,d) impurity (I), excitonic (X), and 3D electron to 2D hole transitions (A, B, C) have been identified.

In the analysis the authors have focused on peak B, which has small overlap with the I and X lines and is related to the SHE. The direct confirmation of SHE behaviour in the LED structure is reproduced in Fig. 14.

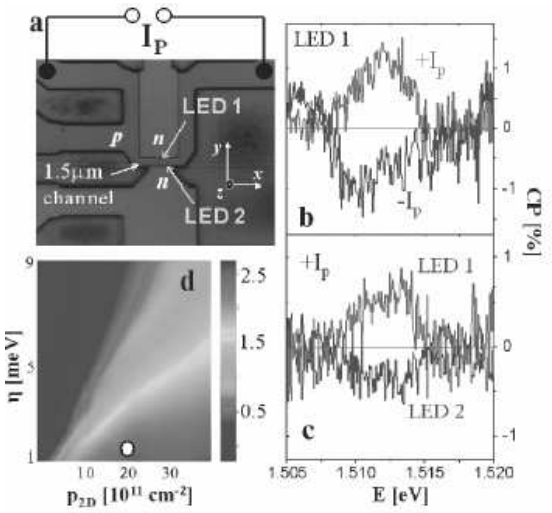

Fig. 14. (a) SEM image of the SHE LED device. (b) Polarization along z axis measured with active LED 1 for two opposite Ip current orientations. (c) Polarization along z axis measured with fixed Ip current and for biased LED 1 or LED 2. (d) Theoretical intrinsic SHE conductivity in units of $e/8\pi$ versus quasiparticle lifetime broadening and 2D hole density. Parameters corresponding to the 2DHG, indicated by a white dot, fall into the strong intrinsic SHE part of the theoretical diagram.

In the SEM image the top (LED 1) or bottom (LED 2) n contacts are shown and they are used to measure the EL at opposite edges of the 2DHG p channel parallel to the SHEdriving current Ip. Nonzero and opposite out-of-plane polarization of peak B of the high bias EL curve of wafer 1 for the two Ip orientations demonstrates the SHE. The data for polarization along z axis measured with fixed Ip current and for biased LED 1 or LED 2 show opposite polarizations at opposite edges of the 2DHG channel, which confirm the SHE origin of the measured signal.

References

[1] I. Zutic, J. Fabian, S. Das Sarma, Rev. Mod. Phys. **76**, 323 (2004).
[2] M. N. Baibich, J. M. Broto, Fert A PRL. **61**, 2472 (1988); G. Binasch, P. Grunberg, F. Saurenbach, W. Zinn, Phys. Rev. B **39**, 4828 (1989).
[3] S. Datta, B. Das, Appl. Phys. Lett. **56**, 665 (1990).
[4] A. Prinz, Science **282**, 1660 (1988).
[5] S. A. Wolf, D. D. Awschalom, Science **294**(2001), 5546 (2001).
[6] International Technology Roadmap for Semiconductors, http:/public.itrs.net .
[7] J. de Boek, W. Van Roy, J. Das, Semicond. Sci. Technol. **17**, 342 (2002).
[8] G. Schmidt, D. Ferrand, L. W. Molenkamp, A. T. Filip, B. van Wees, Phys. Rev B **62**, R4793 (2000).

[9] R. Fiederling, M. Keim, G. Reuscher, W. Ossau, G. Schmidt, A. Waag, L. W. Molenkamp, Nature **402**, 787 (2000).
[10] T. Dietl, H. Ohno, F. Matsukura, J. Cibert, D. Ferrand, Science **287**, 1019 (2000).
[11] G. Birliba, S. Cârlig, V. Kantser, Proc. Fifth General Conference BPU-5 Vrnjacka Banja, Serbia and Montenegro, p. 567, (2003).
[12] R. H. Silsbee, J. Phys.Condens.Matter. **16**, R179 (2004).
[13] D. Bjorken, S. D. Drell, Relativistic Quantum Mechanics (Mc Graw Hill, New York 1964).
[14] Z. Y. Wang, C. D. Xiong, cond-mat/ 0504049.
[15] B. A. Bernevig, cond-mat/0408476.
[16] O. A.Pankratov, JETP Lett **45**, 82 (1987).
[17] V. Kantser, N. M. Malkova, JETP Lett **54**, 388 (1991).
[18] V. Kantser, Mold. Journ Phys. Sci. **4**, 3, (2005).
[19] S. Murakami, N. Nagaosa, S. C. Zhang, Science **301**, 1348 (2003).
[20] J. Sinova, D. Culcer, Q. Niu, N. A. Sinitsyn, T. Jungwirth, A. H. MacDonald, Phys. Rev. Lett. **92**, 126603 (2004).
[21] M. I. D'yakonov, V. I. Perel', JETP Lett. **13**, 467 (1971).
[22] Y. K. Kato, R. C. Myers, A. C. Gossard, D. D. Awschalom, Science **306**, 1910 (2004).
[23] J. Wunderlich, B. Kaestner, J. Sinova, T. Jungwirth, Phys. Rev. Lett. **94**, 047204 (2005).
[24] P. R. Hammar, B. R. Bennett, Yang and Johnson, Mark., PRLett. **83**, 203 (1999).
[25] E. I. Rashba, Phys. Rev. B **62**, R16267 (2000).
[26] V. P. LaBella, D. W. Bullock, Z. Ding, C. Emery, A. Vencatesan, W. F. Oliver, G. J. Salamo, P. M. Thibado, M. Mortazavi, Science **92**, 1518 (2001).
[27] A. T. Hanbicki, B. T. Jonker, G. Itskos, G. Kioseoglou, Petrou, Appl. Phys. Lett. **80**, 1240 (2002).
[28] Masaaki Tanaka, Semicond. Sci. Technol. **17**, 327 (2002).
[29] F. Matsukura, H. Ohno, A. Shen, Y. Sugawara, Phys. Rev. B **57**, R2037 (1998).
[30] T. Dietl, Semicond. Sci. Technol. **17**, 377 (2002).
[31] J. Szczytko, K. Swiatek, M. Palczewska, A. Twardowski, T. Hayashi, M. Tanaka, K. Ando, Phys. Rev. B **60**, 8304 (1999).
[32] J. Kreissl, W. Ulrici, M. El-Metoui, A.-M. Vasson, A. Vasson, A. Gavaix 1996 Phys. Rev. B **54**, 10508 (1996).
[33] K. Sato, H. Katayama-Yoshida, Jpn. J. Appl. Phys. **40** L485 (2001).
[34] M. L. Reed, N. A. El-Masry, Stadelmaier, M. K. Ritmus, M. J. Reed, C. A. Parker, J. C. Roberts, S. M. Bedair, Appl. Phys. Lett. **79**, 3473 (2001).
[35] S. Sonoda, S. Shimizu, T. Sasaki, Y. Yamamoto, H. Hori, J. Cryst. Growth **237-239**, 1358 (2002).
[36] F. Holtzberg, S. von Molnar, J. M. D. Coey, "Handbook on Semiconductors," ed. T. Moss (North-Holland, Amsterdam 149 (1980).
[37] J. M. D. Coey, M. Viret, S. von Molnar, Adv. Phys. **48**, 167 (1999).
[38] J. M. D. Coey, M. Venkatesan, J. Appl. Phys. **91**, 8345 (2002).
[39] J. J.Versluijs, M. A. Bari, J. M. D. Coey, PRL **87**, 6601 (2001).
[40] J. W. Dong, L. C. Chen, C. J. Palmstrom, R. D. James, S. McKernan, Appl. Phys. Lett. **75**, 1443 (1999).
[41] J. Q. Xie, J. W. Dong, J. Lu, C. J. Palmstrom, S. McKernan, Appl.Phys.Lett.**79**, 1003 (2001).
[42] C. T. Tanaka, J. Nowak, J. S. Moodera, J. Appl. Phys. **86**, 6239 (1999).
[43] H. Akinaga, T. Manago, M. Shirai, Jap. J. Appl. Phys. **39**, L1118 (2000).
[44] S. von Molnar, J. Supercond. **16**, 1 (2003).
[45] P. LeClair, J. K. Ha, H. J. M. Swagten, J. T. Kohlepp, C. H. van de Vin, W. J. M. de Jonge, Appl. Phys. Lett. **80**, 625 (2002).
[46] H. Kępa, J. Kutner-Pielaszek, J. Blinowski, Europhys. Lett. **56**, 54 (2001).
[47] G. Sprinholz, T. Schwarzl, W. Heiss, G. Bauer, M. Aigle, H. Pascher, I. Vavra, Appl. Phys. Lett. **79**, 1225 (2001).
[48] A. Belenchuk, O. Shapovalov, V. Kantser, A. Fedorov, P. Schunk, T. Schimmel, Z. Dashevsky, J. Crystal Growth 198/199 (1999) 216.
[49] H. Luo, G. B. Kim, M. Cheon, M. Na, S. Wang, B. D. McCombe, X. Liu, Y. Sasaki, T. Wojtoxicz, J. K. Furdyna, G. Boishin, L. J. Whitmanc, Physica E **20**, 338 (2004).
[50] E. A. de Andrada e Silva, G. C. La Rocca, F. Bassani, Phys. Rev. B **55**, 16 293 (1997).
[51] E. A. de Andrada e Silva, Phys. Rev. B **60**, 8859 (1999).
[52] V. I. Perel, Phys. Rev. B **68**, 19699 (2003).
[53] V. G. Kantser, N. M. Malkova, Phys.Rev. B **56**, 2004 (1997).
[54] D. K. Young, J. A. Gupta, E. Johnston-Halperin, R. Epstein, Y. Kato, D. D. Awschalom, Semicond. Sci. Technol. **17**, 275 (2002).
[55] S. A. Wolf, D. D. Awschalom, R. A. Buhrman, J. M. Daughton, S. von Molnar, M. L. Roukes, A. Y. Chtchelkanova, D. M. Treger, Science **294**, 1488 (2001).
[56] I. Malajovich, J. M. Kikkawa, D. D. Awschalom, J. J. Berry, N. Samarth PRL **84**, 1015 (2000).
[57] J. Fabian, S. Das Sarma, J. Vac. Sc. Technol. B **17**, 1708 (1999).
[58] G. Salis, Y. Kato, K. Ensslin, D. C. Driscoll, A. C. Gossard, D. D. Awschalom, Nature **414**, 619 (2001).
[59] G. Sundaram, Q. Niu, Phys. Rev. B **59**, 14915 (1999).
[60] Shuichi Murakami, cond-mat/ 0405003.
[61] B. Laikhtman, R. A. Kichl, Phys. Rev B **47**, 10515 (1993).
[62] Shuichi Murakami, Naoto Nagaosa, Shou-Cheng Zhang, Phys. Rev B **69**, 235206 (2004).

Corresponding author: kantser@lises.asm.md